Amperometric flow-injection analysis of phenols induced by reactive oxygen species generated under daylight irradiation of titania impregnated with horseradish peroxidase

Article

Amperometric flow-injection analysis of phenols induced by reactive oxygen species generated under daylight irradiation of titania impregnated with horseradish peroxidase

Vanoushe Rahemi, Stanislav Trashin, Zainab Hafideddine, Sabine Van Doorslaer, Vera Meynen, Lo Gorton, and Karolien De Wael

Anal. Chem., **Just Accepted Manuscript** • DOI: 10.1021/acs.analchem.9b04617 • Publication Date (Web): 27 Jan 2020

Amperometric flow-injection analysis of phenols induced by reactive oxygen species generated under daylight irradiation of titania impregnated with horseradish peroxidase

Vanoushe Rahemi[a], Stanislav Trashin[a], Zainab Hafideddine[b,c], Sabine Van Doorslaer[b], Vera Meynen[d], Lo Gorton[e], Karolien De Wael[a]*

[a]AXES Research Group, University of Antwerp, Groenenborgerlaan 171, 2020 Antwerp, Belgium

[b]BIMEF Laboratory, University of Antwerp, Universiteitsplein 1, B-2610 Wilrijk, Belgium

[c]PPES Research Group, University of Antwerp, Universiteitsplein 1, B-2610 Wilrijk, Belgium

[d]Laboratory of Adsorption and Catalysis (LADCA), University of Antwerp, Universiteitsplein 1, B-2610 Wilrijk, Belgium

[e]Department of Analytical Chemistry/Biochemistry and Structural Biology, Lund University, PO Box 124, SE-22100 Lund, Sweden

ABSTRACT: Titanium dioxide (TiO_2) is a unique material for biosensing applications due to its capability of hosting enzymes. For the first time we show that TiO_2 can accumulate reactive oxygen species (ROS) under daylight irradiation and can support the catalytic cycle of horseradish peroxidase (HRP) without the need of H_2O_2 to be present in the solution. Phenolic compounds, such as hydroquinone (HQ) and 4-aminophenol (4-AP), were detected amperometrically in flow-injection analysis (FIA) mode via the use of an electrode modified with TiO_2 impregnated with HRP. In contrast to the conventional detection scheme, no H_2O_2 was added to the analyte solution. Basically, the inherited ability of TiO_2 to generate reactive oxygen species is used as a strategy to avoid adding H_2O_2 in the solution during the detection of phenolic compounds. Electron paramagnetic resonance (EPR) spectroscopy indicates the presence of ROS on titania which, in interaction with HRP, initiate the electrocatalysis towards phenolic compounds. The amperometric response to 4-AP was linear in the concentration range between 0.05 and 2 μM. The sensitivity was 0.51 A M^{-1} cm^{-2} and the limit of detection (LOD) 26 nM. The proposed sensor design opens new opportunities for the detection of phenolic traces by HRP-based electrochemical biosensors, yet in a more straightforward and sensitive way following green chemistry principles of avoiding the use of reactive and harmful chemical such as H_2O_2.

Applications of titanium dioxide (TiO_2) as a photocatalyst [1-3] or catalyst support [4-6] have attracted wide interest over the last decade. More recently, significant attention has been paid to the enhancement and/or extension of the optical absorption properties of TiO_2 to improve its overall activity.[7-11] Indeed, for specific applications it is important to improve the optical absorption of titania for photocatalysis. However, solar daylight can provide 3 to 5% of its radiation intensity within the absorption spectral range of titanium dioxide.[12] Since the energy of the incident photons and less their intensity is of interest for photocatalysis, even ordinary room light may be sufficient to excite titania.[1] Thus, in a well-lit lab, with a total light intensity of ~10 μW cm^{-2}, the intensity of UV light with energy exceeding that of the TiO_2 band gap would be approximately 1 μW cm^{-2}.[1] Therefore, it is not required to use UV light to activate titania. The electrons and holes generated under ordinary room light can produce radical species after reaction with water and oxygen.[13] Hydroxyl radical $^{\bullet}OH$, hydroperoxyl radical $^{\bullet}OOH$ and superoxide ion radical $^{\bullet}O_2^-$ are commonly produced reactive species, which participate in the reduction and oxidation reactions and may act as oxidants.[14]

Next to its ability to generate reactive species to a certain extent, (mesoporous) TiO_2 has good biocompatibility and stability [15,16] and therefore, it is a suitable material to immobilize biomolecules.[17,18] TiO_2-based enzymatic sensors for the determination of phenolic compounds usually comprise tyrosinase [19-21], peroxidase [22-25] or laccase [26-29] enzymes. The working principle of these biosensors is based on the redox cycling of a biocatalytic oxidation product of an analyte and the following electrochemical reduction.[30] Hydrogen peroxide (in case of peroxidases) or oxygen (in case of laccase or tyrosinase) plays the role of an ultimate electron acceptor that continuously regenerates the reactive form of the enzyme.[31] Horseradish peroxidase (HRP) is advantageous for developing phenolic biosensors due to its high catalytic activity towards a broad range of phenols [31,32], but the need of H_2O_2 in the solution complicates the analysis and increases background noise.[33] Therefore, a hydrogen peroxide-less HRP-based biosensor

would create the anticipated solution with important benefits in sensitivity for the detection of phenols.

Herein we use the inherited ability of TiO_2 to generate reactive oxygen species as a strategy to avoid adding H_2O_2 in the solution during the detection of phenolic compounds. We implement this strategy in flow-injection analysis (FIA) because of comparatively short contact time of the sample with the electrode surface and enhanced mass transport in a wall-jet flow cell during amperometric measurements.[34,35] In contrast to our previous studies on analysis of phenols at a TiO_2-HRP modified electrode [23], the sensor in this work can be used as prepared and it does not require any H_2O_2 neither for activation nor operation and it follows green chemistry principles of avoiding the use of reactive and harmful H_2O_2. This is advantageous to all previously described HRP-based sensors for phenols.

EXPERIMENTAL SECTION

Materials

Hydrogen peroxide (H_2O_2), nafion 117 (5% in a mixture of lower aliphatic alcohols and water), potassium chloride (KCl), 4-aminophenol (4-AP), and potassium phosphate monobasic (KH_2PO_4) were purchased from Sigma-Aldrich. Hydroquinone (HQ) was obtained from Acros, TiO_2 (Millennium PC500, mesoporous anatase) from Crystal Global (prior to use, the TiO_2 was calcined to 450 °C to enlarge its pore size).[36] Horseradish peroxidase (HRP) (EC 1.11.1.7) with the activity of 293.0 U/mg was purchased from Calbiochem. 10 mM KH_2PO_4 phosphate buffer and 0.1 M KCl solution (pH 7.0) was used as supporting electrolyte. The spin trap 5-(diethoxyphosphoryl)-5-methyl-l-pyrroline N-oxide (DEPMPO) was purchased from Focus Biomolecules. SBA-15 materials with different pore sizes were synthesized using the amphiphilic triblock copolymer P123.[37] The phosphate buffer solution was set to pH 7.0 using NaOH solution. All reagents were used without further purification and all solutions were prepared with deionized water.

Apparatus

A double line flow-injection system with a three-electrode wall-jet flow-through cell made of plexiglas [38] (Figure S1) was used for the amperometric detection of phenols. A peristaltic pump (Perkin-Elmer, France) propelled the phosphate buffer (pH 7.0) as the carrier into the flow line using Tygon tubing (1 mL/min flow rate). A 50 µL sample solution containing substrate (phenolic compounds) was injected into the carrier stream via a omnifit labware (Diba) manual sample-injection valve (USA). The flow line was made from Teflon tubing (0.75 mm i.d. and 1.59 mm o.d.). A HRP-TiO_2 modified graphite electrode, an Ag/AgCl (0.1 M KCl) electrode, and a platinum wire were used as the working, reference, and auxiliary electrodes, respectively. Electrochemical measurements were carried out using a PalmSens potentiostat (Utrecht, The Netherlands) with PSTrace software (version 5.3). Electrochemical measurements were performed at room temperature. The amperometric measurements were repeated four times for each concentration. For EPR measurements, X-band (~9.44 GHz) continuous-wave (CW) EPR analyses were performed on a Bruker ESP300E spectrometer equipped with a liquid Helium cryostat (Oxford Inc.). The room-temperature EPR spectra (single scan) were recorded with a modulation amplitude of 0.1 mT, microwave power of 10 mW, receiver gain of 2×10^5. The low-temperature EPR spectra were recorded at 10 K, with a modulation amplitude of 0.5 mT and a microwave power of 0.5 mW. For both experiments a modulation frequency of 100 kHz is applied. A vacuum pump was used during the low temperature experiments to remove paramagnetic oxygen from the sample. *In-situ* illumination was done with a MGL-III-532 green DPSS laser and a MDL-III-447 violet blue diode laser. The EPR spectra are simulated using the MATLAB toolbox Easyspin.[39]

Modification of the electrode

The procedure for immobilizing HRP in mesoporous TiO_2 is reported in our previous work.[23] The HRP-containing TiO_2 material is abbreviated as TiO_2-HRP. A rod of spectroscopically pure graphite (diam. 3.05 mm, SPI, Belgium) was modified by drop-casting a suspension (5 µL) containing TiO_2-HRP (10 mg/mL) and nafion (0.05%). The electrode was dried at room temperature in the dark for approximately 1 h. The electrodes are abbreviated as Graphite|TiO_2-HRP. The electrodes not containing HRP are denoted as Graphite|TiO_2.

RESULTS AND DISCUSSION

Graphite|TiO_2-HRP with and without H_2O_2 in the flow for monitoring hydroquinone

HRP catalyses the oxidation of organic substrates, such as phenolic compounds, by H_2O_2 and it can be employed in the amperometric analysis of phenols.[25,40,41] However, the addition of H_2O_2 results in continuous background drift, increased background noise and fluctuation. The problem can be partially solved by generation of H_2O_2 in flow using a flow reactor with glucose oxidase and glucose as a stable molecule that leads to the formation of hydrogen peroxide *in-situ* in the flow when passing the reactor.[42] This solves the problem with long term stability of H_2O_2 but cannot solve issues related to the increased background current and noise since the excess of H_2O_2 is still present in the working solution.

In this work we evaluate the analytical performances of a Graphite|TiO_2-HRP electrode in a wall-jet flow cell of a FIA system for detection of phenols in the presence and absence of H_2O_2 in the cell solution. To minimize the artefacts from possible fluctuations in H_2O_2 concentration during the injection of a sample, we used a two channel pump that mixes a carrier flow with the buffer containing H_2O_2 as shown in Figure 1a. This scheme maintains exactly the same concentration of H_2O_2 during the analysis but dilutes the sample twice and increases twice the flow rate due to combining two flows of the same flow rate. By simple replacement of the H_2O_2 buffer solution by pure buffer we can compare the behaviour of the system with (Figure 1a) and without (Figure 1b) H_2O_2 in the flow, keeping all other parameters unchanged.

Notice that the scheme in Figure 1b is identical to the FIA with one channel (Figure S2) pumped with a double speed and double diluted injected sample (which would be the simplest possible configuration for functioning FIA, if H_2O_2

is not needed). However, we kept the FIA scheme as shown in Figure 1 for accurate comparison between measurements in the presence and absence of H_2O_2. On the contrary, the use of the scheme with two channels (Figure 1a) is necessary in the presence of H_2O_2 to avoid fluctuations in H_2O_2 concentration during injections that would result in artefacts as shown in Figure S3.

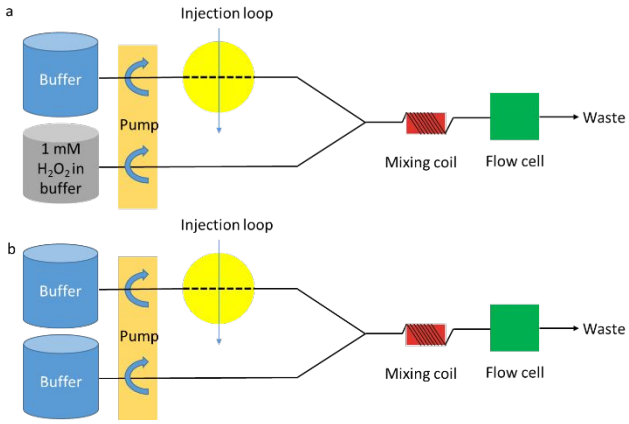

Figure 1. Schematic of the flow-injection system in the presence (a) and absence (b) of H_2O_2 in the carrier stream.

Calibration curves for the detection of HQ were constructed for these two possible FIA configurations (Figure 2). In the low concentration range (0.15 µM-5 µM), Graphite|TiO_2-HRP electrodes did retain the sensitivity to HQ and, even more, showed almost double increase in sensitivity from a value of 0.18 A M^{-1} cm^{-2} in the presence of H_2O_2 to a value of 0.31 A M^{-1} cm^{-2} in pure buffer (in the absence of H_2O_2). However, in the absence of H_2O_2 (Figure S4), the current-concentration profile (Figure 2) reaches a constant value already at 5 µM while it stays near linear till 100 µM in the presence of H_2O_2 (Figure S5) in the cell solution. This limits the performance of Graphite|TiO_2-HRP electrodes in the absence of H_2O_2 by the lower concentration range of hydroquinone, *i.e.* below 5 µM. This is not a critical limitation for developing a sensor since the sub-µM concentration range is the region of interest for the detection of phenolic contaminants. The limits of detection (LOD) were 0.2 µM and 0.33 µM of HQ by taking into account the dilution factor for the flow setup in the absence and presence of H_2O_2, correspondingly.

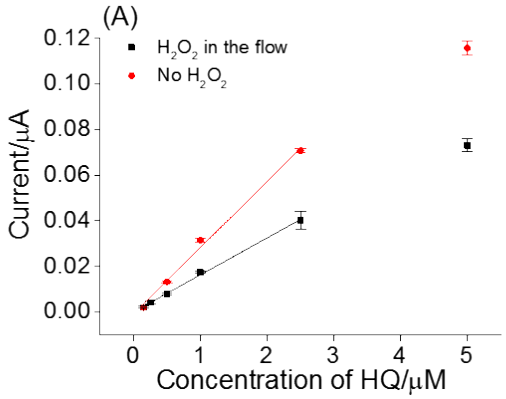

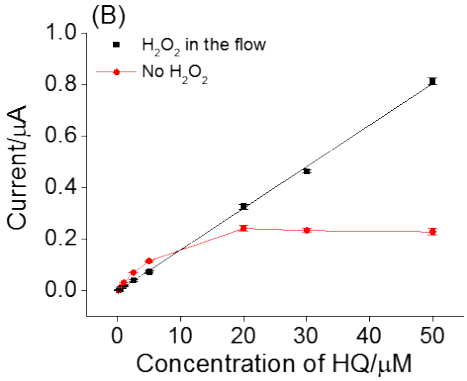

Figure 2. Calibration curve of a Graphite|TiO_2-HRP electrode with 1 mM H_2O_2 in the flow (black) and without 1mM H_2O_2 in the flow (red) for (A) low HQ concentrations (0.15 µM- 5 µM) and (B) high HQ concentration (µM). Applied potential, -0.1 V vs. Ag/AgCl. Flow rate, 1 mL/min.

To confirm the biocatalytic role of HRP in the detection of HQ in the absence of H_2O_2, Graphite|TiO_2 and Graphite|TiO_2-HRP electrodes were compared in the same conditions (Figure S6). Only minor responses comparable to the background noise were measured at Graphite|TiO_2 electrode in the range of 1-5 µM HQ with a current of 1.4 nA for 5 µM HQ, whereas the response at Graphite|TiO_2-HRP electrode was 83 times higher in the same conditions. The significant difference in the sensitivity clearly shows that the signal is specific to the HRP-catalyzed process.

Besides the improved analytical performances of Graphite|TiO_2-HRP electrodes in the absence of H_2O_2, an interesting question rises regarding chemical reactions that support the HRP redox catalysis at TiO_2 surface in the absence of H_2O_2. Obviously, the oxidation of HQ catalysed by HRP, requires a second co-reactant, *i.e.* H_2O_2. But in the absence of H_2O_2 added in the solution, reactive oxygen species (ROS) that are created on the surface of TiO_2 at ambient conditions, may act as the sacrificial oxidant or eventually transform into some amount of H_2O_2, which happens near the site of the enzyme location. EPR studies can clarify details about the appearance of reactive oxygen species on titania.

CW-EPR characterization

Photoexcitation of TiO_2 generates electron-hole pairs which results in conduction-band electrons and valence-band holes. This charge transfer generates paramagnetic species, which can be detected by EPR. The conduction-band electrons can be trapped on diamagnetic Ti^{4+} sites to form paramagnetic Ti^{3+} centres. Holes trapped at localised oxide ions O^{2-} result in the formation of O^- centres. Surface Ti^{3+} centres can interact with O_2 leading to superoxide, O_2^-.[43-45] In turn, surface O^- centres can form O_3^- after interaction with O_2. In addition, Ti^{3+} sites can also react with O_2 and H_2O to form radicals such as •OOH (derived from superoxide) and •OH. Although many reactions are possible with O_2 at the surface, the formation of O_2^- and •OOH is thermodynamically the most favourable.[44] These surface reactive oxygen species (ROS) can then rapidly react with

other molecules, such as proteins present on the titania surface. In this paper, two approaches are applied for the detection of these radicals via EPR. One way is the use of nitrone-based spin traps to trap short-living free radicals with life times at room temperature too short to detect with EPR. By reaction of these radicals with the spin traps, radical spin adducts with longer half-life are formed. The spin trap 5-(diethoxyphosphoryl)-5-methyl-l-pyrroline N-oxide (DEPMPO) is used as a probe for oxy radical formation on the TiO_2 surface.[46] The reaction with O_2^- results in the spin adduct DEPMPO-•OOH which is more persistent than spin adduct of other traps.[46] In this study, PC500 Millenium TiO_2 powder (only anatase as crystal phase) is used for the electrode modification. TiO_2 powder is suspended in a water solution of DEPMPO and measured at room temperature before and during illumination with green light (532 nm) or blue light (447 nm) to understand the effect of the visible part of daylight on TiO_2 (Figure 3).

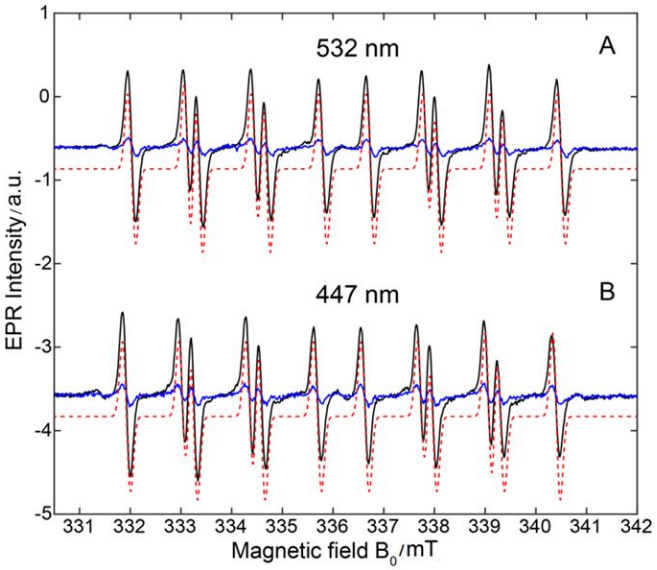

Figure 3. Room-temperature X-band EPR spectra of a suspension of TiO_2 in an aqueous solution of DEPMPO before (blue) and during (black) illumination (A) at 532 nm and (B) at 447 nm. The corresponding simulation of the black spectrum is shown as a dashed line (red) (the simulated spectrum is shown shifted versus the experimental data to allow better spectral comparison).

After two minutes of irradiation the EPR signal intensity increases significantly, revealing the formation of a spin-trapped radical. The EPR spectrum can be simulated with g = 2.0056 and nitrogen, phosphorous, ß- and □-proton hyperfine-coupling constants: a_N = 1.332 mT, a_H^{β} = 1.1166 mT, a_P = 4.710 mT and $a_H^{\gamma} \leq 0.07$ mT (± 0.02), which is typical for the DEPMPO-OOH radical, proving that superoxide has been spin trapped.[46-48] Even though the band gap of titania materials lies in the UV region, a considerable effect is observed when using visible light. The UV-Vis DR spectra seem to indicate no absorption at 447 and 532 nm (Figure S7). The fact that the PC500 Millenium titania produces significant amounts of superoxide during green and blue light illumination may be due to the use of a laser (high light intensity), the presence of a transition-metal ion contamination in the TiO_2 batches (e.g. Fe^{3+}) or the calcination process that induces different defect sites that act as electron acceptors in the band gap. UV-Vis DR may not be sensitive enough to detect the presence of a limited amount of these sites. A similar effect of visible light illumination has been observed previously for other titania.[49]

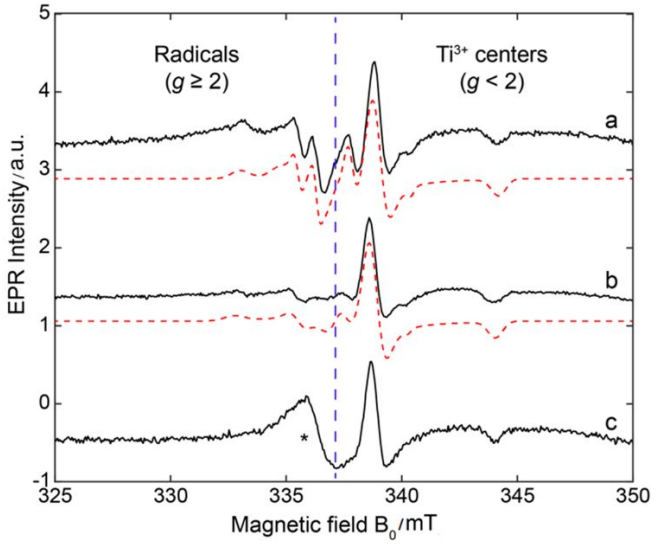

Figure 4. X-band EPR spectrum of the subtraction of the EPR spectrum before illumination from the EPR spectrum during illumination at 532 nm (light-dark) of a) PC500 Millenium TiO_2 powder, b) PC500 Millenium TiO_2 powder in HEPES buffer pH 7 and c) TiO_2-HRP powder in HEPES buffer pH 7 measured at 10 K. The dashed lines show the corresponding simulation using the parameters in Table S1. The blue vertical dashed line indicates the g = 2.00 position.

As the second detection strategy, EPR spectra of the TiO_2 powders and their suspensions are measured at low temperature (10K) without the addition of a spin trap. This is to verify that the DEPMPO spin trap is not responsible for side reactions resulting in the formation of O_2^-. At low temperatures the stability of the photo-induced ROS is increased making them EPR detectable. The EPR spectrum of TiO_2 powder recorded at 10 K in dark reveals the presence of a stable radical with a clear g value around 2.001 (Figure S8b). It is possible that a carbon-containing radical (such as CO_2^-) is present due to insufficient calcination. When the material is dispersed in buffer solution, these signals largely disappear, showing that they mainly stem from surface centers that can react with the buffer molecules and/or are washed off the surface (Figure S8a). In a next step, different TiO_2 samples are illuminated at low temperature with green light (532 nm, Figure 4 and S9) or blue light (447 nm, Figure S10) for 30 minutes to understand the effect of the visible part of daylight on TiO_2. Measurements are done for the PC500 Millenium TiO_2 powder, a suspension of the TiO_2 powder and of the TiO_2-HRP powder, the latter two suspensions in HEPES buffer (pH 7). In all cases, illumination leads to the appearance of an intense axial signal with $g_{\perp}$ = 1.9895 and $g_{\parallel}$ = 1.959, that can be ascribed to anatase bulk Ti^{3+} centers .[50-52] An additional smaller Ti^{3+}-related EPR signal is also observed in the samples without HRP ($g_{\perp}$ = 1.9966 and $g_{\parallel}$ = 1.981).

Moreover, a light-induced broad EPR feature occurs around g = 1.93 in line with the presence of Ti^{3+} surface sites in a disordered environment (Figure S11).[53,54]

Moreover, illumination induces different EPR signals in the spectral region g ≥ 2. These signals can be assigned to organic radicals.[44,45,55-59] Table 1 gives an overview of the detected EPR contributions of these radicals observed in the TiO_2 powders and suspensions and their tentative assignment. A more detailed description is given in the supplementary material. A significant fraction of the light-induced EPR signals can be attributed to formation of superoxide at different surface sites. For O_2^-, the g_z value is very sensitive to changes in the crystal field due to different local coordination on the Ti^{4+} centers.[58,60] The observation of signals at g values larger than 2.02 unambiguously proves the presence of superoxide radicals.

Table 1. g values of the radicals observed on the PC500 TiO_2 surface.

	g_z	g_y	g_x	*Tentative assignment*
Illumination at 532 nm				
TiO_2 powder	2.0350 ± 0.0050	2.0120 ± 0.0030	2.0025 ± 0.0010	O_2^-/•OOH
	2.0248 ± 0.0005	2.0096 ± 0.0003	2.0015 ± 0.0010	O_2^-
	2.0060 ± 0.0015	2.0045 ± 0.0005	2.0030 ± 0.0015	$V_o^{\bullet}$ or C-centered radical
TiO_2 suspension	2.0257 ± 0.0005	2.0096 ± 0.0003	2.0010 ± 0.0010	O_2^-
Illumination at 447 nm				
TiO_2 powder	2.0230 ± 0.0010	2.0096 ± 0.0010	2.0015 ± 0.0010	O_2^-
	2.0330 ± 0.0010	2.0124 ± 0.0010	2.0025 ± 0.0010	O_2^-
	2.0580 ± 0.0050	2.0120 ± 0.0020	2.0030 ± 0.0020	O_2^- (?)
	2.0175 ± 0.0005	2.0130 ± 0.0010	2.0040 ± 0.0010	O_3^-
	2.0060 ± 0.0015	2.0045 ± 0.0005	2.0030 ± 0.0015	$V_o^{\bullet}$ or C-centered radical
TiO_2 suspension	2.0260 ± 0.0003	2.0110 ± 0.0002	2.0030 ± 0.0002	O_2^-

The presence of O_2^- and its protonated form •OOH can lead to the formation of H_2O_2 on the hydroxylated TiO_2 surface, because the superoxide radicals can react with surface hydroxyl groups at the TiO_2 surface. The formed •OOH radicals can dimerise to form H_2O_2, which is EPR silent.[61]

Low-temperature illumination of the TiO_2-HRP system in HEPES buffer reveals again a light-induced response, although the EPR signal of the oxygen-centred radicals is now very broad, indicative of the presence of different radicals making it difficult to simulate accurately (Figure 4c, signal indicated with asterisk and Figure S10c). These experiments are also repeated with the addition of HQ, showing analogue results (Figure S12). As a control HRP was incorporated in a porous silica material (SBA-15), here called HRP-SiO_2. The EPR spectra of HRP-SiO_2 measured before, during and after illumination showed only an intensity difference due to slight detuning in the EPR cavity during illumination, but no spectral changes due to radical formation (Figure S13A). This confirms the unique formation of superoxide in the titania-based systems.

In the low-field area of the EPR spectra of HRP-TiO_2, the high-spin (HS) components of the ferric forms of HRP are clearly visible (Figure S14).[62] It is known that the HS forms of peroxidases are sensitive to the environment, resulting in different HS components in SiO_2 and TiO_2 (Figures S13B and 14).[63] Illumination with green and blue light causes a slight decrease in intensity of these HS signals, which is largely restored after switching off the laser. Since the same effect is observed for HRP-SiO_2 (Figure S13B), a light-induced detuning of the EPR set-up is most likely. Green light is absorbed by the ferric HRP inducing electronic transitions (Q-bands of the absorption spectrum).

Effect of working potential

The effect of working potential on the sensitivity of Graphite|HRP-TiO_2 was studied in the range from +0.2 to -0.4 V in a solution containing 10 µM HQ (Figure 5). The response of a Graphite|TiO_2-HRP electrode proportionally increases as the applied potential shifts towards more negative values, reaching a plateau at -0.2 V. At more negative potential values, the electrochemical reduction of molecular oxygen contributes considerably to the response of the phenolic compound and it may cause a slow irreversible deactivation of adsorbed HRP. A low background current and no influence of oxygen reduction motivates the selection of a working potential of -0.10 V.

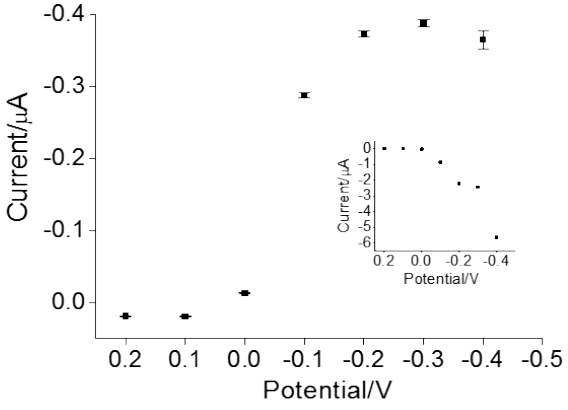

Figure 5. Influence of the applied potential on the amperometric response of 10 µM HQ at Graphite|HRP-TiO_2 in 10 mM phosphate buffer (pH 7.0) containing 0.1 M of KCl. Flow

rate, 1 mL/min. inset: changes in the background current upon applying different potentials.

Applicability of our system

To explore the applicability of the electrode for on-site detections, the amperometric response to 4-aminophenol (4-AP) was measured at E= -0.10 V (Figure S15). As shown in Figure 6, the calibration plot for HRP-TiO_2 is linear in the sub-micromolar concentration range starting to deviate from linearity at 0.5 µM and leveling off above 10 µM. The sensitivity was 0.51 A M^{-1} cm^{-2} in the low-concertation range; and the limit of detection (LOD) was 26 nM calculated as 3 × standard deviation of blank/slope calibration curve. The LOD for 4-AP in the present work is at least four times lower than the reported LOD in the literature for other biosensors in flow system (Table 2) which shows favourable analytical performance of our electrochemical biosensor.

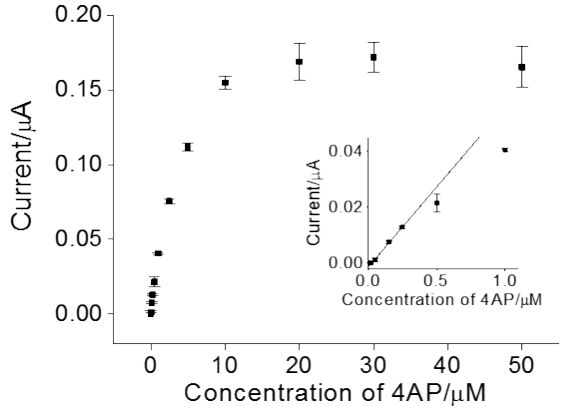

Figure 6. Calibration plot obtained for 4-AP at Graphite|TiO_2-HRP operated without H_2O_2. Inset: lower 4-AP concentration range. Applied potential, -0.1 V vs. Ag/AgCl. Flow rate, 1 mL/min.

Table 2. Comparison of the limit of detection for 4-aminophenol using flow injection analysis.

Method	*LOD (µM)*
This method	*0.026*
Flow system combined with a glucose oxidase-mutarotase reactor in the presence of H_2O_2 [42]	*0.1 ± 0.01*
Flow system combined graphite electrodes modified with laccases [64]	*0.39*
Flow system combined graphite electrodes modified with laccases [65]	*0.37*
Flow system with spectrophotometric detection [66]	*10*
Flow system using chemiluminescence detection [67]	*17.6*
HPLC [68]	*3*

In order to test the practical application of the proposed sensor, TiO_2-HRP was used for the detection of 4-AP in river water. Prior to the analyses, the river water was filtered through a 0.2 µm PES membrane and spiked with 0.05, 0.1 and 0.2 µM 4-AP. During flow-injection analysis the samples are diluted twice by buffer in the mixing coil. The recovery values were calculated using a calibration curve obtained in deionized water in the same concentration range of 4-AP at the same sensor. The recovery was (106 ± 11)%, (96 ± 11)% and (65 ± 6)% for 0.05, 0.1 and 0.2 µM 4-AP, respectively. The high recovery values, especially for the low concentrations, demonstrate the viability of the suggested detection method for real sample analysis.

CONCLUSIONS

For the first time, we used the inherited ability of TiO_2 to generate reactive oxygen species as a strategy to avoid adding H_2O_2 in the solution during the detection of phenolic compounds. In general, horseradish peroxidase (HRP) needs H_2O_2 as an oxidant in the reaction mechanism. It was found that Graphite|TiO_2-HRP electrodes perform better in the absence of H_2O_2 than similar electrodes in the presence of 0.5 mM H_2O_2 in the flow (sensitivity to HQ was 1.7 times higher). The possibility to operate in H_2O_2 free buffer was caused by the presence of reactive oxygen species (ROS) at the surface of TiO_2. At the optimum conditions for HQ, the electroanalytical behaviour of Graphite|TiO_2-HRP for 4-aminophenol (4-AP) was studied and compared with reported data related to 4-AP in literature by using flow injection analysis. This work opens new opportunities for HRP based sensors functioning without H_2O_2 and capable to measure phenols in the sub-µM concentration range by flow injection analysis.

ASSOCIATED CONTENT

Supporting Information

The Supporting Information containing additional EPR characterization and amperometry measurements in detail is available free of charge on the ACS Publications website.

AUTHOR INFORMATION

Corresponding Author

* Karolien De Wael, karolien.dewael@uantwerpen.be.

ACKNOWLEDGMENT

The authors thank Scientific Research-Flanders (FWO) (grant 12T4219N) for funding.

REFERENCES

(1) Fujishima, A.; Rao, T. N.; Tryk, D. A. *Journal of Photochemistry and Photobiology C: Photochemistry Reviews* **2000**, *1*, 1-21.

(2) Fujishima, A.; Zhang, X. *Comptes Rendus Chimie* **2006**, *9*, 750-760.

(3) Nakata, K.; Fujishima, A. *Journal of Photochemistry and Photobiology C: Photochemistry Reviews* **2012**, *13*, 169-189.
(4) Do, T. B.; Cai, M.; Ruthkosky, M. S.; Moylan, T. E. *Electrochimica Acta* **2010**, *55*, 8013-8017.
(5) Kaneko, E. Y.; Pulcinelli, S. H.; Teixeira da Silva, V.; Santilli, C. V. *Applied Catalysis A: General* **2002**, *235*, 71-78.
(6) Rebrov, E. V.; Berenguer-Murcia, A.; Skelton, H. E.; Johnson, B. F. G.; Wheatley, A. E. H.; Schouten, J. C. *Lab on a Chip* **2009**, *9*, 503-506.
(7) Chen, X.; Mao, S. S. *Chemical reviews* **2007**, *107*, 2891-2959.
(8) Ma, Y.; Wang, X.; Jia, Y.; Chen, X.; Han, H.; Li, C. *Chemical reviews* **2014**, *114*, 9987-10043.
(9) Chen, X.; Liu, L.; Yu, P. Y.; Mao, S. S. *Science* **2011**, *331*, 746-750.
(10) Miao, F.; Wang, Z.; Tao, B.; Chu, J.; Chu, P. K. *Electrochimica Acta* **2013**, *112*, 32-36.
(11) Szkoda, M.; Trzciński, K.; Nowak, A. P.; Coy, E.; Wicikowski, L.; Łapiński, M.; Siuzdak, K.; Lisowska-Oleksiak, A. *Electrochimica Acta* **2018**, *278*, 13-24.
(12) Pârvulescu, V. I.; Marcu, V. In *Surface and Nanomolecular Catalysis*, Richards, R., Ed.; CRC Press, 2006, pp 427-460.
(13) Xie, Q.; Zhao, Y.; Chen, X.; Liu, H.; Evans, D. G.; Yang, W. *Biomaterials* **2011**, *32*, 6588-6594.
(14) Lu, S.-y.; Wu, D.; Wang, Q.-l.; Yan, J.; Buekens, A. G.; Cen, K.-f. *Chemosphere* **2011**, *82*, 1215-1224.
(15) Zheng, W.; Zheng, Y. F.; Jin, K. W.; Wang, N. *Talanta* **2008**, *74*, 1414-1419.
(16) Paddon, C. A.; Marken, F. *Electrochemistry Communications* **2004**, *6*, 1249-1253.
(17) Dai, Z.; Yan, F.; Chen, J.; Ju, H. *Analytical Chemistry* **2003**, *75*, 5429-5434.
(18) Liu, S.; Chen, A. *Langmuir* **2005**, *21*, 8409-8413.
(19) Kochana, J.; Wapiennik, K.; Kozak, J.; Knihnicki, P.; Pollap, A.; Wozniakiewicz, M.; Nowak, J.; Koscielniak, P. *Talanta* **2015**, *144*, 163-170.
(20) Liu, X.; Yan, R.; Zhu, J.; Zhang, J.; Liu, X. *Sensors and Actuators B: Chemical* **2015**, *209*, 328-335.
(21) Yu, J.; Liu, S.; Ju, H. *Biosensors and Bioelectronics* **2003**, *19*, 509-514.
(22) Kafi, A. K. M.; Chen, A. *Talanta* **2009**, *79*, 97-102.
(23) Rahemi, V.; Trashin, S.; Meynen, V.; De Wael, K. *Talanta* **2016**, *146*, 689-693.
(24) Calza, P.; Avetta, P.; Rubulotta, G.; Sangermano, M.; Laurenti, E. *Chemical Engineering Journal* **2014**, *239*, 87-92.
(25) Yu; Ju. *Analytical Chemistry* **2002**, *74*, 3579-3583.
(26) Kochana, J.; Nowak, P.; Jarosz-Wilkołazka, A.; Bieroń, M. *Microchemical Journal* **2008**, *89*, 171-174.
(27) Hou, J.; Dong, G.; Ye, Y.; Chen, V. *Journal of Membrane Science* **2014**, *469*, 19-30.
(28) Jia, J.; Zhang, S.; Wang, P.; Wang, H. *Journal of Hazardous Materials* **2012**, *205-206*, 150-155.
(29) Hou, J.; Dong, G.; Ye, Y.; Chen, V. *Journal of Membrane Science* **2014**, *452*, 229-240.
(30) Marko-Varga, G.; Emnéus, J.; Gorton, L.; Ruzgas, T. *TrAC Trends in Analytical Chemistry* **1995**, *14*, 319-328.
(31) Yang, S.; Li, Y.; Jiang, X.; Chen, Z.; Lin, X. *Sensors and Actuators B: Chemical* **2006**, *114*, 774-780.
(32) Lindgren, A.; Emnéus, J.; Ruzgas, T.; Gorton, L.; Marko-Varga, G. *Analytica Chimica Acta* **1997**, *347*, 51-62.
(33) Trashin, S.; Rahemi, V.; Ramji, K.; Neven, L.; Gorun, S. M.; De Wael, K. *Nature Communications* **2017**, *8*, 16108.
(34) Trojanowicz, M.; Szewczynska, M.; Wcislo, M. *Electroanalysis* **2003**, *15*, 347-365.
(35) Yaropolov, A. I.; Kharybin, A. N.; Emnéus, J.; Marko-Varga, G.; Gorton, L. *Analytica Chimica Acta* **1995**, *308*, 137-144.
(36) Ribbens, S.; Beyers, E.; Schellens, K.; Mertens, M.; Ke, X.; Bals, S.; Van Tendeloo, G.; Meynen, V.; Cool, P. *Microporous and Mesoporous Materials* **2012**, *156*, 62-72.
(37) Yu, C.; Fan, J.; Tian, B.; Zhao, D.; Stucky, G. D. *Advanced Materials* **2002**, *14*, 1742-1745.
(38) Appelqvist, R.; Marko-Varga, G.; Gorton, L.; Torstensson, A.; Johansson, G. *Analytica Chimica Acta* **1985**, *169*, 237-247.
(39) Stoll, S.; Schweiger, A. *Journal of magnetic resonance (San Diego, Calif. : 1997)* **2006**, *178*, 42-55.
(40) Rosatto, S. S.; Sotomayor, P. T.; Kubota, L. T.; Gushikem, Y. *Electrochimica Acta* **2002**, *47*, 4451-4458.
(41) Yang, S.; Chen, Z.; Jin, X.; Lin, X. *Electrochimica Acta* **2006**, *52*, 200-205.
(42) Munteanu, F.-D.; Lindgren, A.; Emnéus, J.; Gorton, L.; Ruzgas, T.; Csöregi, E.; Ciucu, A.; van Huystee, R. B.; Gazaryan, I. G.; Lagrimini, L. M. *Analytical Chemistry* **1998**, *70*, 2596-2600.
(43) Xiong, L.-B.; Li, J.-L.; Yang, B.; Yu, Y. *Journal of Nanomaterials* **2012**, *2012*, 1-13.
(44) Carter, E.; Carley, A. F.; Murphy, D. M. *The Journal of Physical Chemistry C* **2007**, *111*, 10630-10638.
(45) Attwood, A. L.; Murphy, D. M.; Edwards, J. L.; Egerton, T. A.; Harrison, R. W. *Research on Chemical Intermediates* **2003**, *29*, 449-465.
(46) Frejaville, C.; Karoui, H.; Tuccio, B.; Moigne, F. L.; Culcasi, M.; Pietri, S.; Lauricella, R.; Tordo, P. *Journal of Medicinal Chemistry* **1995**, *38*, 258-265.
(47) Dikalov, S.; Landmesser, U.; Harrison, D. G. *The Journal of biological chemistry* **2002**, *277*, 25480-25485.
(48) Dikalov, S.; Jiang, J.; Mason, R. P. *Free Radical Research* **2005**, *39*, 825-836.
(49) Hurum, D. C.; Agrios, A. G.; Gray, K. A.; Rajh, T.; Thurnauer, M. C. *The Journal of Physical Chemistry B* **2003**, *107*, 4545-4549.
(50) Kus, M.; Altantzis, T.; Vercauteren, S.; Caretti, I.; Leenaerts, O.; Batenburg, K. J.; Mertens, M.; Meynen, V.; Partoens, B.; Van Doorslaer, S.; Bals, S.; Cool, P. *The Journal of Physical Chemistry C* **2017**, *121*, 26275-26286.
(51) Macdonald, I. R.; Rhydderch, S.; Holt, E.; Grant, N.; Storey, J. M. D.; Howe, R. F. *Catal Today* **2012**, *182*, 39-45.
(52) Livraghi, S.; Chiesa, M.; Paganini, M. C.; Giamello, E. *The Journal of Physical Chemistry C* **2011**, *115*, 25413-25421.
(53) Chiesa, M.; Paganini, M. C.; Livraghi, S.; Giamello, E. *Physical Chemistry Chemical Physics* **2013**, *15*, 9435-9447.
(54) Rajh, T.; Ostafin, A. E.; Micic, O. I.; Tiede, D. M.; Thurnauer, M. C. *The Journal of Physical Chemistry* **1996**, *100*, 4538-4545.
(55) Anpo, M.; Che, M.; Fubini, B.; Garrone, E.; Giamello, E.; Paganini, M. C. *Top Catal* **1999**, *8*, 189-198.
(56) Green, J.; Carter, E.; Murphy, D. M. *Chemical Physics Letters* **2009**, *477*, 340-344.
(57) Carter, E.; Carley, A. F.; Murphy, D. M. *Chemphyschem : a European journal of chemical physics and physical chemistry* **2007**, *8*, 113-123.
(58) Srinivas, D.; Manikandan, P.; Laha, S. C.; Kumar, R.; Ratnasamy, P. *Journal of Catalysis* **2003**, *217*, 160-171.
(59) Nakaoka, Y.; Nosaka, Y. *Journal of Photochemistry and Photobiology A: Chemistry* **1997**, *110*, 299-305.
(60) Che, M.; Tench, A. J. In *Advances in Catalysis*, Eley, D. D.; Pines, H.; Weisz, P. B., Eds.; Academic Press, 1983, pp 1-148.
(61) Diesen, V.; Jonsson, M. *The Journal of Physical Chemistry C* **2014**, *118*, 10083-10087.
(62) Blumberg, W. E.; Peisach, J.; Wittenberg, B. A.; Wittenberg, J. B. *Journal of Biological Chemistry* **1968**, *243*, 1854-1862.
(63) Svistunenko, D. A.; Worrall, J. A. R.; Chugh, S. B.; Haigh, S. C.; Ghiladi, R. A.; Nicholls, P. *Biochimie* **2012**, *94*, 1274-1280.
(64) Haghighi, B.; Jarosz-Wilkołazka, A.; Ruzgas, T.; Gorton, L.; Leonowicz, A. *International Journal of Environmental Analytical Chemistry* **2005**, *85*, 753-770.
(65) Haghighi, B.; Gorton, L.; Ruzgas, T.; Jönsson, L. J. *Analytica Chimica Acta* **2003**, *487*, 3-14.
(66) Bloomfield, M. S. *Talanta* **2002**, *58*, 1301-1310.
(67) Xu, H.; Duan, C.-F.; Zhang, Z.-F.; Chen, J.-Y.; Lai, C.-Z.; Lian, M.; Liu, L.-J.; Cui, H. *Water Research* **2005**, *39*, 396-402.

(68) Zhang, S. S.; Liu, H. X.; Yuan, Z. B. *Journal of Chromatography B: Biomedical Sciences and Applications* **1998**, *705*, 165-170.

For Table of Contents Only